# The 6-Hz wave measurements in Western Java Sea and its preliminary characteristics analysis

[1]Dian Adrianto, [2]Eko B. Djatmiko, [2]Suntoyo

[1] Post Graduate Program, Faculty of Marine Technology, Institut Teknologi Sepuluh Nopember (ITS), Surabaya, Indonesia; [2] Department of Ocean Engineering, Institut Teknologi Sepuluh Nopember (ITS), Surabaya, Indonesia. Corresponding author: D. Adrianto, aqilaadrianto@gmail.com

**Abstract**. The need for wind wave data derived from direct measurements in the field in various sea areas in Indonesia is considered very urgent to be done, although various methods of predicting and analyzing sea waves from secondary data have been carried out to meet these needs. The sea wave measurement program in the West Java Sea has been comprehensively carried out for one full year. The device used is the MUSD (Modified Ultra Sonic Device) which is a modification tool of the ultrasonic sensor-based sea level elevation device which was previously used in tidal recording. Modifications were made by replacing some components so that a 6 Hz sampling frequency is achieved. The device was installed on an oil wellhead platform operated by CNOOC Southeast Sumatra Ltd. The collected data are grouped every 30 minutes in order to get 48 wave group per day. The short-term of wave statistical method and its spectrum has been employed to perform preliminary analysis. The results of the analysis provide the distributions and characteristic values of wave elevation, height and period, as well as patterns of the corresponding wave energy spectra. The average wave height ratios of *Hs*/*Hav* = 1.735, *Hs*/*Hrms* = 1.422, and *Hmax*/*Hs* = 1.856 are derived from the analysis. These ratios are in conformation with the ranges as suggested by prominent references.
**Key Words**: wave, direct measurement, statistical analysis, spectral analysis, Western Java Sea.

**Introduction**. In general, wave theories are used to predict ocean structure responses to wave excitations, assuming that the waves are regular. For an initial study the application of regular wave theory to explore ocean structure behaviors, accommodated in a deterministic mathematical model, is acceptable. However, for actual design the application of regular wave theory is not appropriate. This is because the sea wave has random characteristics in nature, hence the ocean structure operated in it will also behave randomly. In this respect further process and analysis on the sea waves should be performed, involving the application of mathematical and statistical methods to derive the short-term and the long-term wave data as well as wave spectral formulae to be implemented in the actual design of ocean structures (Chakrabarti 1987).

The wave data and spectral formulae for the seas in developed countries are already well established and widely available. In the field of marine technology, especially in the facet of design and operation of seagoing ships and ocean structures, the wave data collection has been pioneered by the British Ship Research Association (BSRA) in the UK and by the David W Taylor Naval Ship Research and Development Center (DTNSRDC) in the USA, notably from the beginning of the 20$^{th}$ century. Following this and in the effort of intensively making use of the ample collected wave data, in the early 1950s Pierson & Marks (1952) introduced the formulation of wave spectra. This is further enhanced and implemented in the study of ship motions in random waves by Denis & Pierson (1953). From the aforementioned exploration and studies it was then understood that a random wave is the result of superposition of a large number, or theoretically infinite number, of regular waves (Cartwright & Longuret-Higgins 1956). Thus ocean waves can be said to have statistical regularity, which means that the more observations performed, the statistical regularity will be seen more clearly.

The development of sea wave spectra formulations has grown more intensively, especially after the introduction of fast Fourier transform algorithm by Cooley & Tukey (1965). The acknowledged sea wave spectral formulae are among others Pierson-Moskowitz (P-M) spectrum, Bretschneider spectrum, and ITTC/ISSC spectrum (Djatmiko 2012; Ryabkova et al 2019). As those spectra are developed to model open sea waves, notably derived for the Atlantic Ocean, then an initiative to study the spectra of closed waters was promoted. This in particular was organized by the countries attached to the North Sea, hence designated as the Joint North Sea Wave Project or widely known as JONSWAP (Hasselman et al 1973, 1976). A more recent study has been explained by Xie et al (2019) in the development of wave spectrum for the northern South China Sea. Here the sea spectrum data from observation is compared to seven types of ocean wave spectrum models. The result of comparison shows that the JONSWAP spectrum with a certain peak enhancement factor agree well with the observed data of South China Sea.

Referring to the above development, Indonesia despite its status as the world largest archipelagic country has not had that kind of privilege in collecting wave data and developing specific wave spectra on its waters. As a developing country comprehensive wave data collection in Indonesia has not been viable in view of the budget limitation and the lack of coordination among the relevant institutions to run a corresponding national program (Djatmiko & Adrianto 2013). Therefore, the requirement in wave data for Indonesian waters to date is supplied mainly from the information provided by the Meteorology, Climatology and Geophysics Agency (BMKG). The information is acquired from data harvesting by means of satellites such as GEOSAT-ALT. The original data harvested by satellites are mostly in the form of wind intensities and directions, which should be processed further to generate wave data.

For some general purposes the wave data generated as aforementioned might be considered appropriate. But for specific applications, such as simulations, predictions, and analyses of ship and ocean structure dynamic behaviors a more detailed wave data should be made available (Djatmiko et al 2019; Murdjito et al 2020). The detailed data as required should cover the time histories of wave elevation which exhibit distinct pattern inherent to certain sea regions. This will only be possible if the wave data collection is carried out by direct measurement with relatively low sampling time interval and performed at reasonably long period. The overall wave time history so accumulated in a long period will then be split into shorter time histories and processed further to produce the wave spectra formulation.

In the effort of meeting the above need, a direct wave measurement program has been initiated under a personally funded research (Adrianto et al 2019). The measurement was carried out at a station in Western Java Sea. A Modified Ultra Sonic Device (MUSD) with a sampling frequency of 6.0 Hz was utilized in a fully one-year long wave data collection, installed on an oil wellhead platform operated by CNOOC Southeast Sumatra Ltd. The wave data processing has then been conducted, involving the short-term wave statistical and wave spectral analyses. Preliminary results of the data processing and analysis, comprises of 48 wave data sets derived from a 1-day measurement, are presented and discussed in this paper. The primary goal of this program is to obtain the wave spectral model suitable for the Western Java Sea, and provide the long-term wave scatter data of this sea area. The success of the current program is expected to strongly promote the more intensive wave measurement program nationwide to be conducted by relevant institutions. The available long-term wave data and spectral models of various sea areas in Indonesia certainly will have a great impact in the design of ships and offshore platforms and the safety of their operations in the region.

## Material and Method

***Direct wave measurement program.*** Various methods in fulfilling wave data direct measurements are still practiced these days. For example, measurements using tools based on pressure and ocean currents (Kun et al 1999), or those that use 3-wave gauges as a fix station (Boccotti 2015). Furthermore, according to technological developments,

several measurements by adopting more advanced technology include the use of Synthetic Aperture Radar (SAR) (Lin et al 2008) or the Advanced Synthetic Aperture Radar (ASAR), with a camera or video (Fedele et al 2013) and satellite images are continuously to be developed.

Having mentioned the above fact, an intensive direct wave measurement program has been carried out at Western Java Sea for a fully one year, starting from June 2016 to June 2017. A Modified Ultra Sonic Device (MUSD) was utilized, by installing it on an offshore platform at a certain height above the sea level. The device is accommodated in a compact data acquisition system (DAS) supported with a digital recording appliance and high-density storage apparatus powered by a solar cell mechanism.

As widely known in its operation the ultrasonic-based device is emitting sound wave at a high frequency directed to the sea surface and receiving the reflected sound from the sea surface. The distance of sea surface to the device is then measured based on the elapsed time from the sound emitted up to the reflected sound is captured (Widjiati et al 2015). The contour of the sea surface elevation can then be generated as the time history of the fluctuation in the time required to emit and reflect sound waves at a given time interval and recorded for certain period of time.

***Location and measurement points***. The location of this research is in the waters of the western part of Java Sea. The measuring device was installed at the Wave Station on an offshore oil wellhead platform at coordinates of 05°27′00.36" S - 106°15"17.51" E, within the Cinta oil and gas field owned by the China National Offshore Oil Corporation (CNOOC) Southeast Sumatra Ltd.. The supporting wind data was obtained from a nearby Meteorological Station located on Pabelokan Island, which also belongs to the same company. Figure 1 shows the lay out locations of the Wave and Meteorological (Wind) stations at the Western Java Sea map.

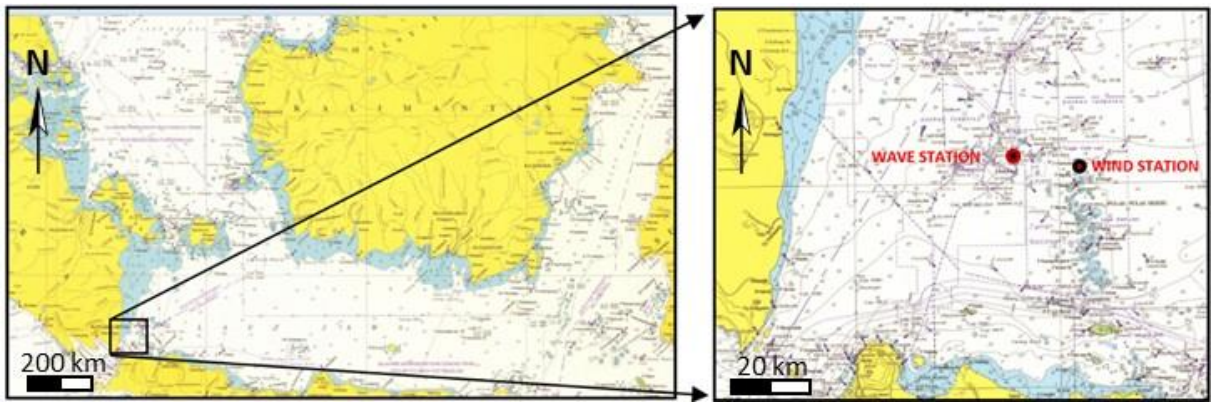

Figure 1. The location of wave and wind stations at Western Java Sea (INHOC 2010).

***The accumulated data***. In the current program the data to establish sea surface elevation time history is obtained with a sampling rate of 6 Hz. Therefore, every 1.0 minute span of acquisition some 360 point data are collected and within 1.0 hour a total of 21,600 data is acquired, or in the extent of 518,400 data in one day. Within a year of 365-day operation practically surface elevation data in the excess of $1.89 \times 10^8$ unit has been collected.

Those overall data were then grouped for every 30 minutes or 0.5 hours, and plotted in the form of time history, containing of 10,800 data points. In this respect for each day there were 48 data groups or surface elevation time histories generated, and within 365 days as much as 17,520 time histories were accumulated.

***Raw data filtering***. In general, the results of wave data recording obtained from direct field measurements contain noises, so filtering is necessary to reduce or even eliminate noise altogether. Hence the data to be analyzed further is wave history data without any noise. Savitzky-Golay Filter (SGF) or also called Digital Smoothing Polynomial Filter (DSPF) and Least Square Digital Filter (LSDF) is used in the current data filtering process.

A very broad low pass filter is used to smooth out noisy signals without distorting much the raw time history data.

Compared to other filters such as Moving Average (MA), SGF has better performance even though the use of MA is simpler and easier (Azami et al 2012). Various uses include improving sound quality during speech (Shajeesh et al 2012) and in the biomedical field SGF has better performance for waves with sharp peaks or stratified waves (Dai et al 2017). Time series data obtained from 1 year measurement were smoothed using the SGF available in the Matlab 2016 toolbox.

***Short-term wave statistical analysis***. After filtering is accomplished, each time history is then analyzed by implementing the short-term wave statistical method (Monbet et al 2007; Guedes-Soares & Carvalho 2012). The first stage of this analysis is conducted to produce the distributions of wave elevation, height and period. In the second stage, by referring to the produced distributions, the characteristic values of wave height and period are computed.

In the case of wave elevation, the distribution is obtained by, firstly, taking values of the wave elevation data from the time history that has been filtered. Theoretically the amount of wave elevation data so acquired will not change from the original data, namely 10,800 unit. The elevation data is distinguished between the elevation above the datum line as positive elevation and elevation below the datum line as the negative elevation. Next the elevation data is grouped to certain interval and plotted in a distribution graph or histogram.

For the case of wave number *N* in each time history, counting is conducted by differentiating between single wave measured from consecutive of one crest to the next crest points (denoted by subscript *c*), one trough to the next trough points (denoted by subscript *t*), one zero up crossing to the next zero up crossing points (denoted by *zu*), and one zero down crossing to the next zero down crossing points (denoted by *zd*), as shown in Figure 2. It should be noted herein, the determination of the number of the wave using the zero-crossing approach is made by taking the intersection of the wave line with the base line used for the starting point and end point of the counting. As indicated in Figure 2(b) in most cases the crossing point, either in the case of zero up or zero down, is not always found exactly at a single recorded data point. Thus, it should be determined from accounting for two sequential recorded points above and below the datum.

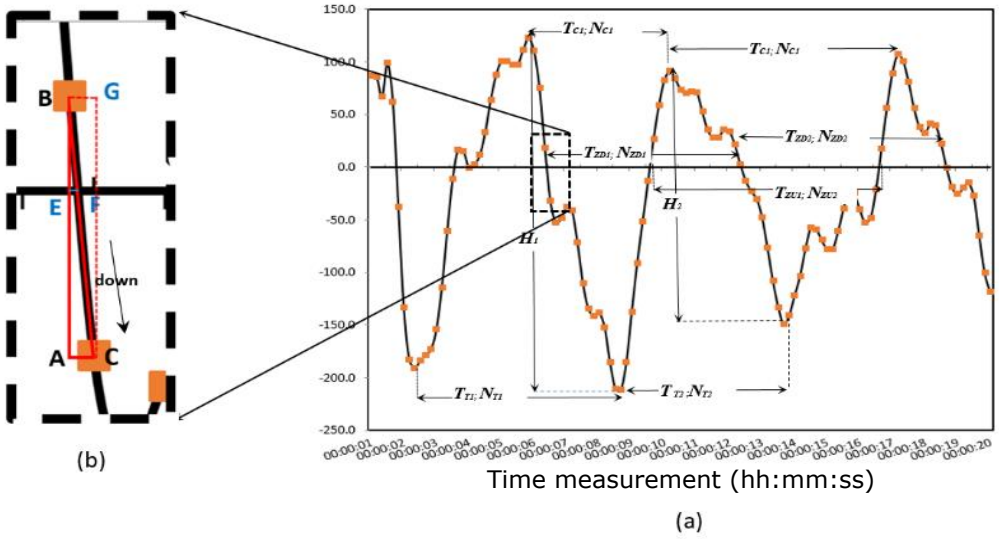


Figure 2. a) Convention in determining *N*, *H* and *T*; b) Convention in determining the zero-crossing scheme *zu* (up) dan *zd* (down).

In Figure 2(b) there are two identical triangles, namely Δ-ABC and Δ-EBF. Points A and C are wave elevation data points at the time of sequential data collection with a time difference of δ*t* or $t_{AC}$ of 0.167 seconds. Point F is the point 0 referred to in this computation. To determine the time of F ($t_F$) it takes the time in B ($t_B$) plus the time difference between point E and point F or $t_{EF}$. This can be written in an equation of:

$$t_F = t_B + t_{EF} \tag{1}$$

where $t_B = t_E = t_A$. Furthermore, with the comparison method of two identical triangles above, it can be written that BE : BA = BF : BC = EF : AC, where the height of BE is $\zeta_k$ and the height of EA is $\zeta_{k+1}$ with $k$ = 1.2 .... N, i.e. the sequential elevation values. It can therefore be written:

$$t_{EF} = 0.167 \frac{\zeta_k}{\zeta_k + |\zeta_{k+1}|} \tag{2}$$

Substitutions of equation (2) into equation (1) results in the following equation:

$$t_F = t_B + \left(0.167 \frac{\zeta_k}{\zeta_k + |\zeta_{k+1}|}\right) \tag{3}$$

Equation (3) can then be written in term of zero down crossing as:

$$t_{ZDk} = t_k + \left(0.167 \frac{\zeta_k}{\zeta_k + |\zeta_{k+1}|}\right) \tag{4}$$

Following this the wave height is measured from any wave crest to the subsequent wave trough. A specific program has been written to pick up the digital data from the time history to measure all the contained wave heights, then grouped into certain wave height interval and finally plotted in the form of wave height histogram. Further, by referring to the wave heights that has been obtained, the values of characteristic wave height comprises of average ($H_{av}$), significant ($H_s$) and root mean square ($H_{rms}$) are obtained by applying equation (5), (6), and (7), with *i* is designated as the *i*-th wave in the time history. In addition to this, the maximum wave height ($H_{max}$) from any single time history is taken as the highest of all the obtained wave heights.

$$H_{av} = \frac{1}{N}\sum_{i=1}^{N} H_i \tag{5}$$

$$H_s = \frac{3}{N}\sum_{i=1}^{N/3} H_i \tag{6}$$

$$H_{rms} = \left[\frac{1}{N}\sum_{i=1}^{N} H_i^2\right]^{1/2} \tag{7}$$

Further, the wave period in the current analysis is differentiated into four types, namely those measured on the basis of consecutive crests ($T_c$), consecutive troughs ($T_t$), consecutive zero up crossing ($T_{zu}$), and consecutive zero down crossing ($T_{zd}$), as shown in the convention of Figure 2. Proceeding equation (4), hence the $T_{zu}$ and $T_{zd}$ can be derived to be identical equation as follows:

$$T_{zdk} = t_{zdk} - t_{zd(k+1)} \tag{8}$$

and

$$T_{zuk} = t_{zuk} - t_{zu(k+1)} \tag{9}$$

The establishment of the wave period histogram is carried out in the same manner as that for wave elevation and wave height. The main values to be determined are the averages of the four type of wave period. Taking *x* as variable to represent *c*, *t*, *zu*, and *zd*, the average of wave period can be found by:

$$\bar{T}_x = \frac{1}{N}\sum_{i=1}^{N} T_{xi} \tag{10}$$

***Wave spectral analysis***. It is widely recognized that random signal such as exhibited by the time history of real sea wave elevation is composed of superposition of a large number, or theoretically infinite number, of harmonic signals or regular wave elevations. In this respect the understanding on the characteristics of the regular wave components that contribute in the formation of random wave is essential. The corresponding general equation of a random wave elevation built up from infinite regular waves may be written as:

$$\zeta(t) = \sum_{i=1}^{\infty} \zeta_{0i} \sin(2\pi\, f_i\, t + \varepsilon_i) \tag{11}$$

where $\zeta(t)$ is the wave elevation at time $t$, $\zeta_0$ is the wave amplitude, $f$ is the wave frequency, and $\varepsilon$ is the wave phase angle, $i$ is $i$-th regular wave component.

The time histories accumulated from the current direct wave measurement are analyzed by applying the well-known fast Fourier transform (FFT) algorithm to establish the associated wave spectra (Hamilton 2010; Cho et al 2015). To some extent results of the spectral analysis will be correlated to the parameters derived from the short-term wave statistical analysis.

## Results and Discussions

***Data recording results***. In this paper discussion is mainly put forward based on the results of preliminary analysis conducted for the wave data accumulated within one day. The data selected was the one recorded on August 13th, 2016 starting from 00:00:00 to 24:00:00 Western Indonesian Time. The one day data was fragmented at every 30 minute interval into 48 sets of wave time history. Group numbers were then used to indicate the set of time history; for instance Group-1 is the time history for data taken at 00:00:01 – 00:30:00, and Group-48 is the time history taken at 23:30:01 – 24:00:00.

A typical initial wave time history is exemplified in Figure 3, which is the one denoted as Group-1. It is immediately notable that the initial data contains noises at some degree. This initial data was then processed for filtering or refinement by employing the SGF algorithm available in the Matlab 2016 toolbox. The result of smoothening process for 1.0-minute span is displayed in Figure 4, where the raw data is shown in the curve with black color, while the smoothed data is the overlaid curve with red color. The graph from filtering indicates the degree of polynomial and the number 31 states the length of the data used. Further, the curve from data filtering for 5.0-minute time span is presented in Figure 5.

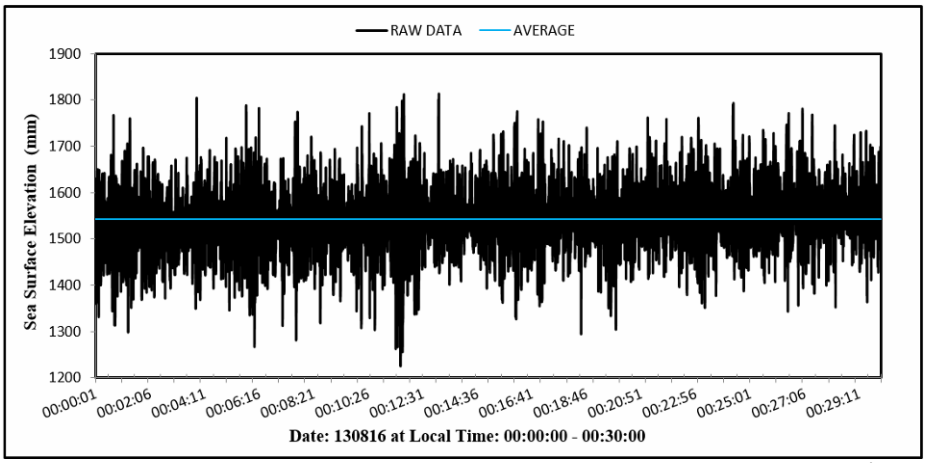


Figure 3. Time history of sea surface elevation recorded on August 13th, 2016 at 00:00:00 – 00:30:00.

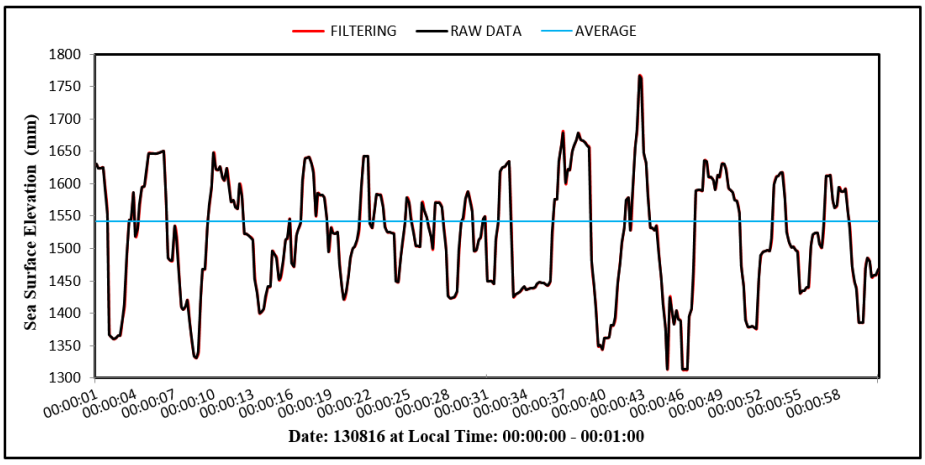


Figure 4. Overlay of sea surface elevation graphs between raw data and data after filtering for 1.0-minute time span.

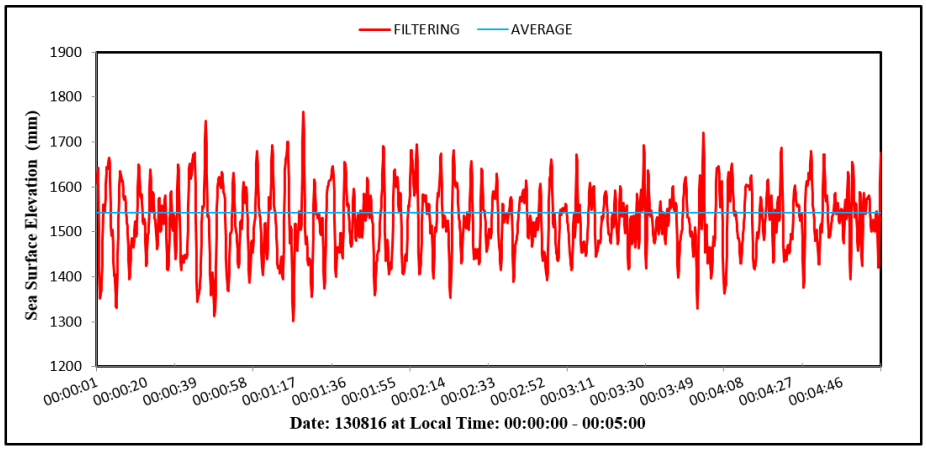


Figure 5. Time history of sea surface elevation recorded after filtering on August 13th, 2016 at 00:00:00 – 00:05:00.

***Distribution of the wave elevation***. Analysis of 48 groups of wave elevation is carried out to determine the frequency distribution of events through analysis of the entire wave elevation histogram. Figure 6 is an example of wave elevation histogram at four (4) prime times that are considered to represent and would show changes in the patterns. The primary times comprise the midnight or Group-1 (00:00:01 – 00:30:00), morning or Group-13 (06:00:01 – 06:30:00), midday or Group-25 (12:00:01 – 12:30:00), and dusk (18:00:01 – 18:00:30).

The abscissa of Figure 6 is the wave elevation interval set at 40 mm and the ordinate is the number of events. As expected, the four graphs exhibit the distributions that resemble the theoretical normal or Gaussian distribution as suggested by Goda (1985).

From the Figure 6 it also can be seen that oscillation occurs in the distribution of higher wave elevations, which experience an increase in the number of events as time of observation increases. This is indicated by the decreasing of the peak of the Gaussian distribution as shown in Figure 6 (a) - 6 (c). Within one day or 24-hour measurement, the lowest decline in the Gaussian distribution occurs at 10:00:00 - 10:30:00 or in the group 21 (not shown in the figure). Then, the distribution gradually returns toward the initial pattern as shown by the increasing peak of the Gaussian distribution in Figure 6(d).

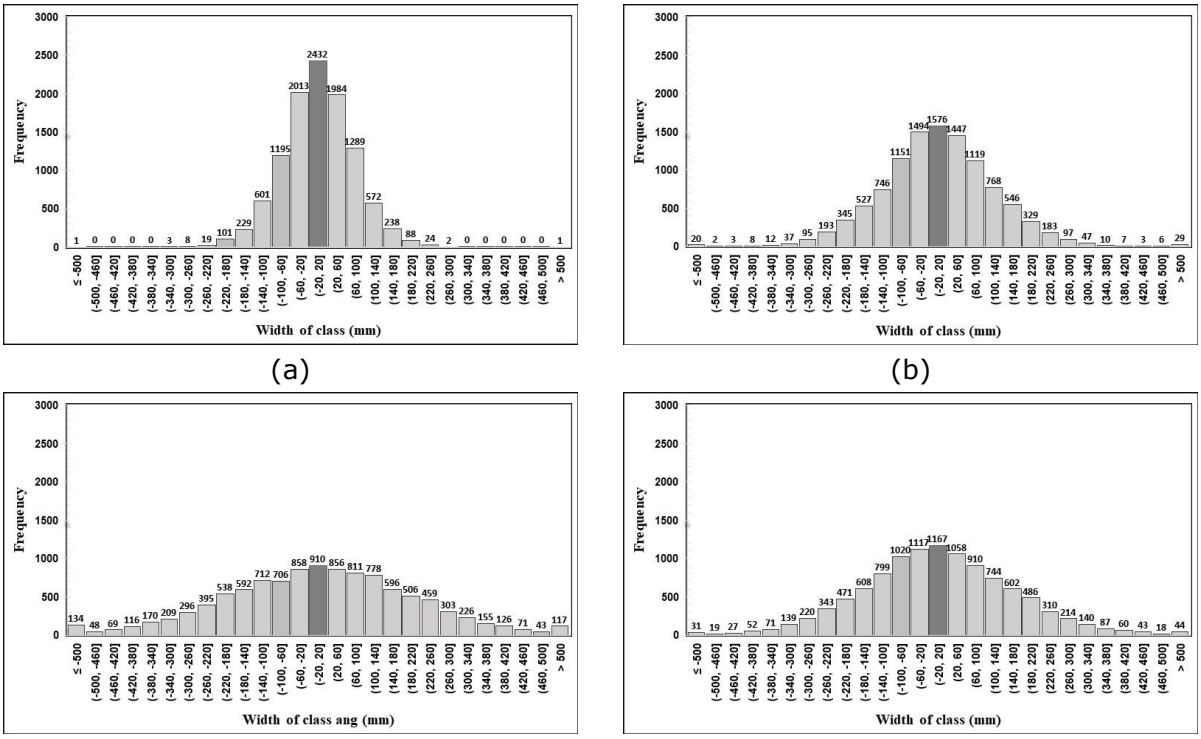


Figure 6. Histograms of the wave elevation for (a) Group-1, (b) Group-13, (c) Group-25 and (d) Group-37.

***Distribution of the wave height***. As previously described, the wave height is determined from the absolute sum of successive crest and trough of a single wave as illustrated in Figure 2(a). The wave height is obtained from the absolute sum of successive crest and trough of a single wave. Then, the results of the computation of wave height distribution in one day or 24 hours measurements are shown as exemplified in Figure 7, which are the histogram of wave height at four (4) prime times that are considered to represent and would show changes in the patterns.

Figure 7 presents the wave height histogram that was established with bin interval of 40 mm and composed up to the last bin containing the wave heights that have values > 1000 mm. From overall the histogram obtained it could be concluded that these resemble the theoretical Rayleigh distribution. This essentially is in agreement with the reference given by Goda (1985) and Chakrabarti (1987). From the Figure 7 it can also be seen that an oscillation occurs in the distribution on the number of events for higher waves in one day, which is eventually increasing in parallel to the increase in observation time. This is characterized by the shift in the Rayleigh peak towards the higher wave heights, as shown in Figures 7 (a) and 7 (b). In one day or 24 hours measurement, the number of events is relatively similar in almost all the wave height classes, particularly in the event between 10:00:00 - 12:30:00 or groups 21-25. Then, the distribution gradually returns to its initial pattern which exhibits by the rising of peak in the Rayleigh distribution at lower wave heights, as portrayed in Figure 7(d).

***Distribution of the wave period***. Figure 8 conveys the wave period histogram that was established with a bin interval of 0.5 seconds and composed up to the last bin containing the wave periods that have values > 7.0 seconds.

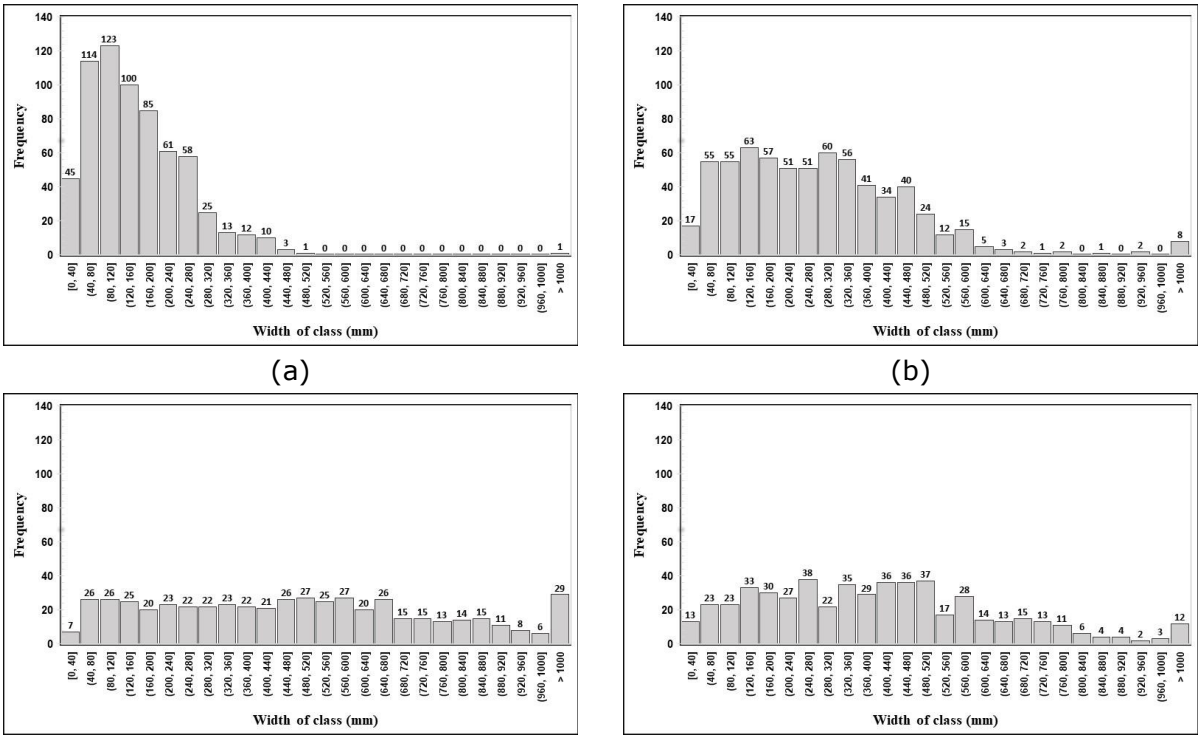


Figure 7. Histograms of the wave height for (a) Group-1, (b) Group-13, (c) Group-25 and (d) Group-37.

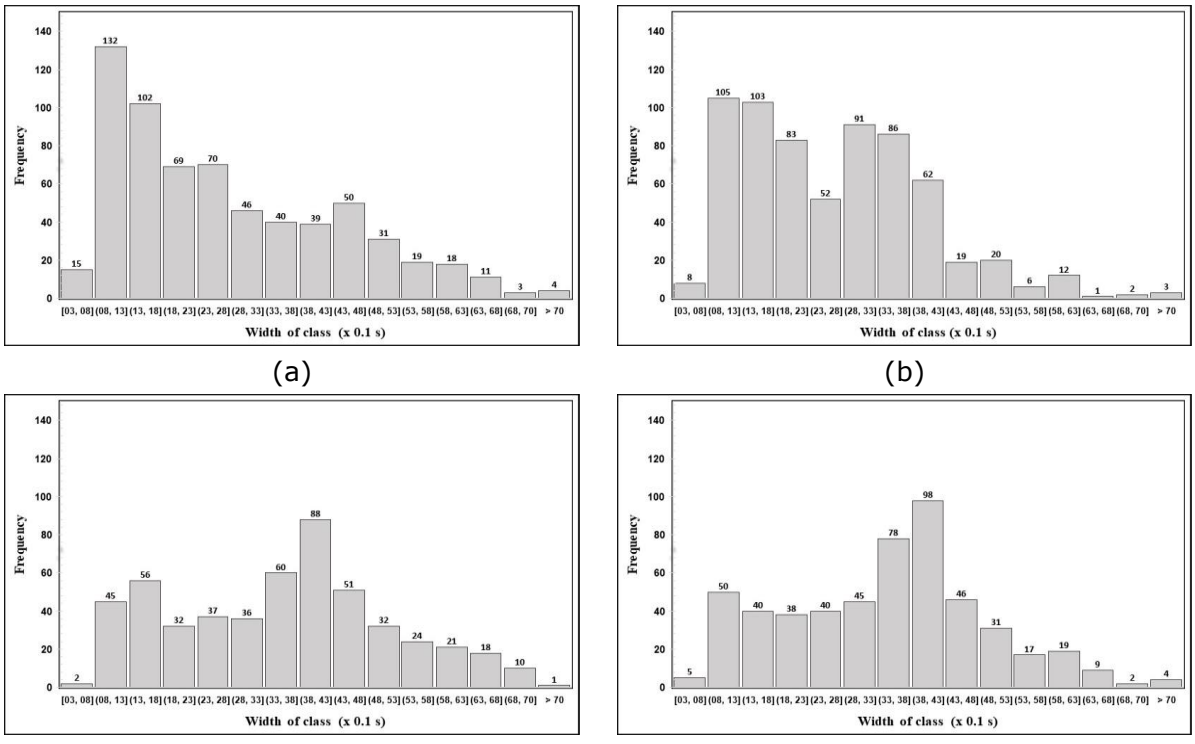


Figure 8. Histograms of the wave period for (a) Group-1, (b) Group-13, (c) Group-25 and (d) Group-37.

By observing the frequency of occurrence of all the data in Groups 1-13 taken from 00:00:01 to 06:30:00 then the dominant wave period is found in classes of 0.8-1.8 seconds. Subsequently, in Groups 14-41 or between 06:30:01-20:30:00 it is dominated by class widths of 3.5-3.8 seconds and 3.8-4.3 seconds. Furthermore, for other groups

the wave periods in class width of 0.8-1.8 seconds dominates again as in the initial observation. It should be noted that throughout the day the frequency of events with the class width of 0.8-1.8 seconds dominates the event more than the width of the other classes, followed by the period class width of 3.8-4.3 seconds. Overall, the distribution of wave periods is in accordance with theoretical exponential family distribution (Goda 1985).

***Results of computation on wave parameters***. The results of computation the number of wave events, wave period values and wave height values of each measurement group are presented in Table 1. The computations were carried out using equations (1) - (11). For the computation of the number and period of waves four (4) approaches were applied as described in the sub-sections above. The computation of wave height provides the values of average value $H_{av}$, root mean square value $H_{rms}$, and significant value $H_s$ obtained from equations (5), (6) and (7) based on the data contained in the time histories. On the other hand, the maximum wave height value $H_{max}$ is acquired from the largest wave height reading from each time history curve.

***The number of waves***. Determination of the number of waves was carried out by adopting four (4) approaches namely crest to crest, trough to trough, and consecutive zero up and down crossing. These are denoted as $N_c$, $N_t$, $N_{zu}$, and $N_{zd}$. The information of the number of waves is needed, among others, to determine the average value of wave height and period. The number of waves recorded in conjunction with every wave data group can be seen in Table 1. This table shows that the number of wave events from 48 measurement groups are in the range of values between 463 and 718 waves. It is known that the sampling frequency is 6.0 Hz so that if each wave group has a time span of 30 minutes and it is formed from 10,800 wave elevations, then each wave has been formed from some 15-23 wave elevation data. The number of waves can to certain extent indicate the band with characteristic of the wave group. The magnitude of the sampling rate in the direct measurement of sea waves also affects the wave type with a smaller period, in addition it also affects the smoothness of the wave cycle pattern so generated. From the computational results, the number of wave events derived from the four (4) approaches in Figure 9 shows a very high correlation with a similarity approaching 100%. In other words, the four approaches show good consistency.

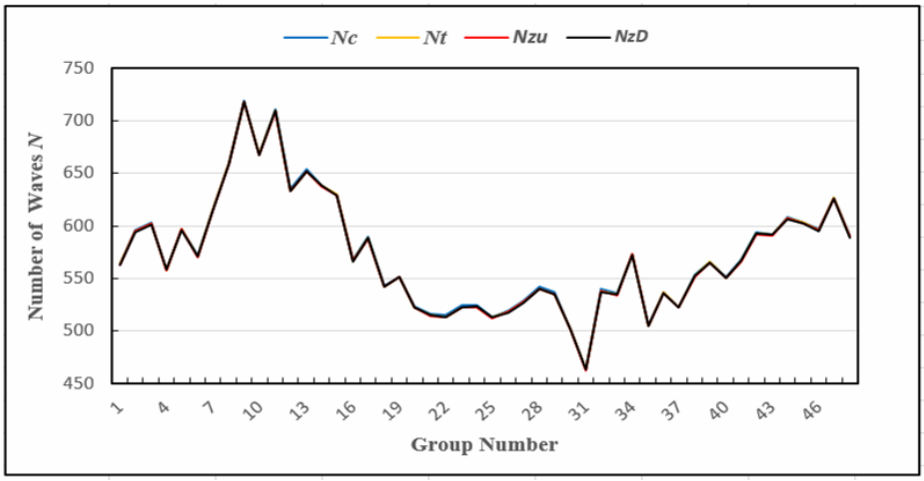


Figure 9. The correlation graphics of 4 approaches in determining number of waves from data collected on August 13th, 2016.

Further, in Figure 9 it can be seen that the shape of the curve has a pattern roughly resembles a sinusoid with one crest and one trough. The crest of the curve lies between Groups 9-12 or between at 04:30:00 and 06:00:00 local time, and the trough lies between Groups 31-32 or at 15:00:00 - 16:00:00 local time.

Table 1

Results of computation on the number of waves, average periods and characteristic heights of waves recorded on August 13th, 2016

| Group | Time | Nc | Nt | Nzu | Nzd | Tc | Tt | Tzu | Tzd | Hav | Hrms | Hs | Hmax |
|---|---|---|---|---|---|---|---|---|---|---|---|---|---|
| | | | | | | Seconds | | | | | Millimeters | | |
| 1 | 00:00:01 - 00:30:00 | 564 | 564 | 563 | 563 | 3,196 | 3,190 | 3,190 | 3,192 | 169 | 288 | 318 | 539 |
| 2 | 00:30:01 - 01:00:00 | 596 | 595 | 595 | 594 | 3,019 | 3,020 | 3,017 | 3,019 | 175 | 220 | 311 | 619 |
| 3 | 01:00:01 - 01:30:00 | 603 | 602 | 602 | 601 | 2,984 | 2,981 | 2,983 | 2,983 | 185 | 245 | 339 | 700 |
| 4 | 01:30:01 - 02:00:00 | 558 | 558 | 558 | 559 | 3,200 | 3,228 | 3,226 | 3,225 | 194 | 249 | 350 | 656 |
| 5 | 02:00:01 - 02:30:00 | 597 | 597 | 597 | 596 | 3,008 | 3,012 | 3,008 | 3,011 | 186 | 244 | 341 | 684 |
| 6 | 02:30:01 - 03:00:00 | 572 | 571 | 570 | 571 | 3,148 | 3,146 | 3,142 | 3,148 | 196 | 251 | 357 | 696 |
| 7 | 03:00:01 - 03:30:00 | 616 | 616 | 615 | 615 | 2,920 | 2,920 | 2,918 | 2,919 | 217 | 291 | 400 | 1057 |
| 8 | 03:30:01 - 04:00:00 | 660 | 660 | 659 | 659 | 2,730 | 2,726 | 2,726 | 2,729 | 234 | 295 | 417 | 1104 |
| 9 | 04:00:01 - 04:30:00 | 719 | 718 | 718 | 718 | 2,503 | 2,501 | 2,501 | 2,499 | 222 | 263 | 379 | 662 |
| 10 | 04:30:01 - 05:00:00 | 668 | 668 | 667 | 667 | 2,694 | 2,693 | 2,695 | 2,694 | 248 | 301 | 430 | 718 |
| 11 | 05:00:01 - 05:30:00 | 711 | 710 | 709 | 710 | 2,530 | 2,532 | 2,530 | 2,530 | 242 | 298 | 420 | 788 |
| 12 | 05:30:01 - 06:00:00 | 635 | 633 | 633 | 633 | 2,838 | 2,838 | 2,835 | 2,835 | 270 | 327 | 466 | 797 |
| 13 | 06:00:01 - 06:30:00 | 654 | 652 | 652 | 652 | 2,750 | 2,749 | 2,750 | 2,749 | 287 | 352 | 493 | 1229 |
| 14 | 06:30:01 - 07:00:00 | 638 | 638 | 637 | 638 | 2,818 | 2,819 | 2,816 | 2,819 | 360 | 440 | 628 | 1111 |
| 15 | 07:00:01 - 07:30:00 | 629 | 630 | 629 | 629 | 2,852 | 2,853 | 2,852 | 2,853 | 370 | 452 | 650 | 1204 |
| 16 | 07:30:01 - 08:00:00 | 568 | 567 | 567 | 566 | 3,166 | 3,168 | 3,167 | 3,167 | 412 | 509 | 727 | 1371 |
| 17 | 08:00:01 - 08:30:00 | 590 | 589 | 588 | 589 | 3,051 | 3,052 | 3,050 | 3,052 | 404 | 498 | 710 | 1515 |
| 18 | 08:30:01 - 09:00:00 | 543 | 542 | 542 | 542 | 3,316 | 3,316 | 3,316 | 3,318 | 474 | 579 | 821 | 1484 |
| 19 | 09:00:01 - 09:30:00 | 552 | 551 | 551 | 551 | 3,258 | 3,260 | 3,260 | 3,260 | 459 | 542 | 782 | 1036 |
| 20 | 09:30:01 - 10:00:00 | 524 | 522 | 522 | 522 | 3,440 | 3,442 | 3,440 | 3,440 | 469 | 560 | 806 | 1259 |
| 21 | 10:00:01 - 10:30:00 | 516 | 515 | 514 | 515 | 3,490 | 3,488 | 3,489 | 3,488 | 510 | 619 | 889 | 1539 |
| 22 | 10:30:01 - 11:00:00 | 515 | 513 | 513 | 513 | 3,494 | 3,495 | 3,495 | 3,492 | 536 | 643 | 920 | 1372 |
| 23 | 11:00:01 - 11:30:00 | 525 | 523 | 523 | 523 | 3,433 | 3,437 | 3,434 | 3,437 | 512 | 629 | 910 | 1788 |
| 24 | 11:30:01 - 12:00:00 | 525 | 523 | 523 | 524 | 3,430 | 3,433 | 3,432 | 3,434 | 520 | 638 | 898 | 1589 |
| 25 | 12:00:01 - 12:30:00 | 513 | 513 | 512 | 513 | 3,507 | 3,506 | 3,507 | 3,507 | 498 | 600 | 856 | 1320 |
| 26 | 12:30:01 - 13:00:00 | 519 | 518 | 518 | 517 | 3,469 | 3,472 | 3,472 | 3,472 | 506 | 603 | 848 | 1336 |
| 27 | 13:00:01 - 13:30:00 | 529 | 528 | 528 | 527 | 3,403 | 3,397 | 3,401 | 3,398 | 458 | 544 | 771 | 1515 |
| 28 | 13:30:01 - 14:00:00 | 542 | 540 | 540 | 540 | 3,326 | 3,326 | 3,325 | 3,327 | 427 | 518 | 756 | 1438 |
| 29 | 14:00:01 - 14:30:00 | 537 | 535 | 535 | 535 | 3,356 | 3,358 | 3,358 | 3,359 | 482 | 594 | 842 | 1452 |
| 30 | 14:30:01 - 15:00:00 | 501 | 501 | 501 | 501 | 3,588 | 3,589 | 3,586 | 3,588 | 489 | 586 | 833 | 1424 |
| 31 | 15:00:01 - 15:30:00 | 464 | 463 | 462 | 463 | 3,879 | 3,878 | 3,875 | 3,879 | 500 | 593 | 832 | 1053 |
| 32 | 15:30:01 - 16:00:00 | 540 | 538 | 538 | 537 | 3,340 | 3,342 | 3,343 | 3,340 | 401 | 486 | 673 | 1124 |

| | | | | | | | | | | | | | |
|---|---|---|---|---|---|---|---|---|---|---|---|---|---|
| 33 | 16:00:01 - 16:30:00 | 536 | 535 | 534 | 535 | 3,359 | 3,356 | 3,354 | 3,356 | 429 | 500 | 721 | 1306 |
| 34 | 16:30:01 - 17:00:00 | 573 | 573 | 573 | 572 | 3,138 | 3,138 | 3,140 | 3,139 | 454 | 546 | 796 | 1002 |
| 35 | 17:00:01 - 17:30:00 | 506 | 505 | 505 | 505 | 3,558 | 3,560 | 3,558 | 3,559 | 458 | 533 | 754 | 978 |
| 36 | 17:30:01 - 18:00:00 | 537 | 537 | 536 | 536 | 3,354 | 3,351 | 3,353 | 3,353 | 431 | 503 | 723 | 1096 |
| 37 | 18:00:01 - 18:30:00 | 523 | 522 | 522 | 522 | 3,443 | 3,443 | 3,442 | 3,444 | 405 | 475 | 680 | 791 |
| 38 | 18:30:01 - 19:00:00 | 554 | 553 | 552 | 553 | 3,250 | 3,249 | 3,248 | 3,249 | 370 | 442 | 637 | 724 |
| 39 | 19:00:01 - 19:30:00 | 566 | 566 | 565 | 565 | 3,182 | 3,179 | 3,183 | 3,181 | 334 | 400 | 571 | 725 |
| 40 | 19:30:01 - 20:00:00 | 551 | 550 | 550 | 550 | 3,266 | 3,269 | 3,269 | 3,267 | 326 | 383 | 551 | 797 |
| 41 | 20:00:01 - 20:30:00 | 568 | 567 | 566 | 567 | 3,166 | 3,166 | 3,166 | 3,166 | 293 | 349 | 502 | 680 |
| 42 | 20:30:01 - 21:00:00 | 594 | 593 | 592 | 593 | 3,031 | 3,029 | 3,029 | 3,031 | 267 | 322 | 459 | 731 |
| 43 | 21:00:01 - 00:30:00 | 592 | 592 | 591 | 592 | 3,036 | 3,039 | 3,036 | 3,037 | 250 | 301 | 432 | 1027 |
| 44 | 21:30:01 - 22:00:00 | 608 | 607 | 607 | 606 | 2,962 | 2,953 | 2,959 | 2,952 | 245 | 305 | 430 | 792 |
| 45 | 22:00:01 - 22:30:00 | 603 | 603 | 602 | 602 | 2,986 | 2,983 | 2,987 | 2,986 | 248 | 317 | 440 | 1002 |
| 46 | 22:30:01 - 23:00:00 | 597 | 596 | 596 | 595 | 3,017 | 3,019 | 3,018 | 3,020 | 244 | 309 | 438 | 1089 |
| 47 | 23:00:01 - 23:30:00 | 627 | 627 | 626 | 626 | 2,867 | 2,867 | 2,867 | 2,865 | 211 | 275 | 381 | 730 |
| 48 | 23:30:01 - 00:00:00 | 591 | 590 | 590 | 589 | 3,047 | 3,049 | 3,049 | 3,049 | 227 | 293 | 400 | 773 |

Based on Figure 9 it can also be analyzed that in one day or 24 hours the number of waves also experiences oscillations from large amounts to small amounts in accordance with the time that mentioned earlier. Generally larger number of waves will correlate with waves having shorter periods and lower heights (Guedes-Soares & Carvalho 2012).

***Wave height intensities***. Figure 10 is an overlay of graphs of the characteristic wave heights $H_{av}$, $H_{rms}$, $H_s$ and $H_{max}$ plotted based on the data from Table 1. There are similarities in the pattern of changes in the curve values of the four characteristic wave heights, which are somewhat close to sinusoid. The curve gradually rises from the midnight measurement time and reaches a peak in Groups 22-25, which is between 10:30:00 and 12:30:00. Then the curve gradually decreases in the afternoon and further in the evening.

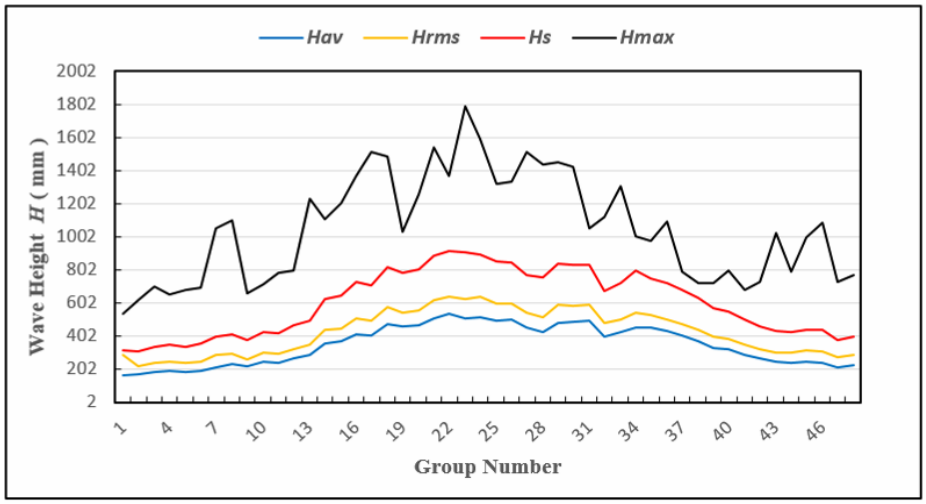


Figure 10. Graphs of $H_{av}$, $H_{rms}$, $H_s$ and $H_{max}$ values obtained from data collected on August 13th, 2016.

The lowest value of average wave height $H_{av}$ is 169 mm and the highest is 538 mm, and the overall mean value is 350 mm. The lowest value of mean square root wave height $H_{rms}$ is 220 mm and the highest is 643 mm, and the overall mean value is 427 mm. The lowest significant wave height value of $H_s$ is 311 mm and the highest is 920 mm, and the overall mean value is 606 mm. The lowest maximum wave height value is 539 mm and the highest is 1788 mm, and the overall mean value is 1050 mm. Then from the overall results in Table 1 it is obtained the correlation between $H_s/H_{av}$ is 1.735, $H_s/H_{rms}$ is 1.422, and $H_{max}/H_s$ is 1.856. These values are in accordance with the general reference which suggests that the range of $H_s/H_{av}$ is in the values between 1.55 amd 1.75, $H_s/H_{rms}$ between 1.35 and 1.5, and $H_{max}/H_s$ between 1.6 and 2.0 (Goda 1985; Chakrabarti 1987).

***Wave period values***. It was explained earlier that the determination of the wave periods for the crest to crest and trough to trough can be directly obtained through the digital reading of the recorded wave data. Though, an initial computation is needed in determining the wave zero-crossing periods, as illustrated in Figure 2(b) and the computation is performed using equation (1) – (4). Basically, the computation of the period is based on four (4) approaches producing high similarity values, having an error approximately < 0.1 seconds.

The results of the computation of the average period from four (4) approaches for 48 complete wave groups can be seen in Table 1. From the table it is proven that the results of the computation on the average period are relatively the same or in other words produce a similarity of values close to 100%. The similarity of value correlations can also be seen in Figure 11. This fact also indicates that all the 48 time histories taken on August 13th, 2016 contain essentially narrow band waves.

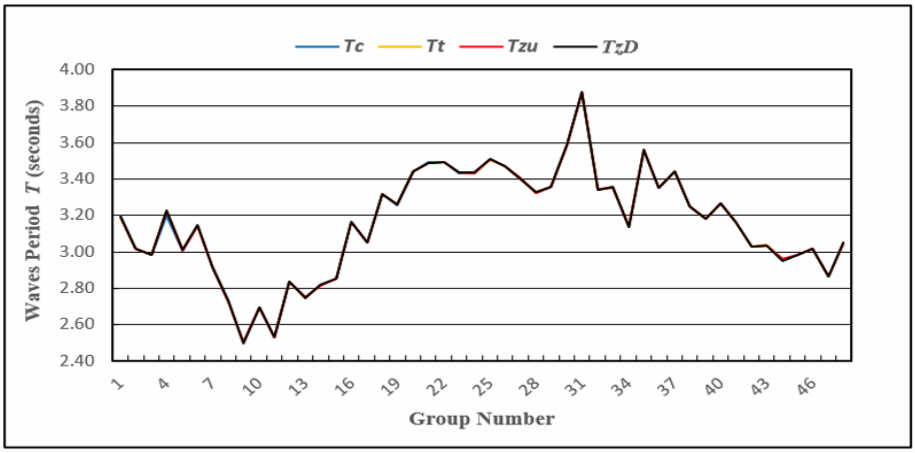


Figure 11. The correlation graphics of 4 approaches in determining wave periods from data collected on August 13th, 2016.

Furthermore, from Table 1 it is known that the average period value ranges between 2.5 and 3.9 seconds. Referring to range of period in the sea wave spectrum chart from Weisse & von Storch (2009), it can be concluded that the current one day data taken on August 13th, 2016 is categorized in the Ordinary Gravity Waves group.

***Results on the wave spectra***. Sea waves are inherently random waves which are formed from the superposition of infinite number regular waves. As mentioned before one of the methods of wave analysis is through the wave energy spectrum obtained from Fourier transformation of the wave record. The transformation is from the time-series function into the frequency domain function.

Figure 12 contains four examples of wave spectra selected from of 48 groups of wave time history, which was processed by FFT. The wave spectra of Group-1 may be approximated by a 1-peak spectral curve, while the other spectra for Group-13, -25, and -37 may be approximated by 2-peak spectral curves.

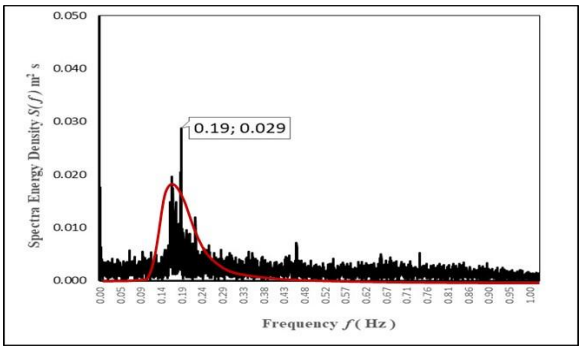


(a)

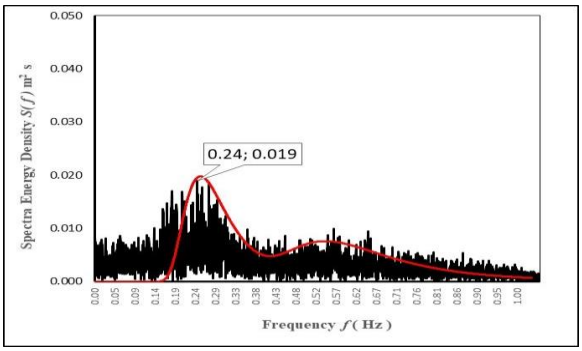


(b)

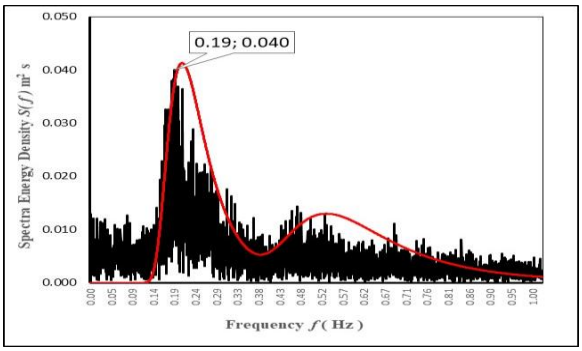


(c)

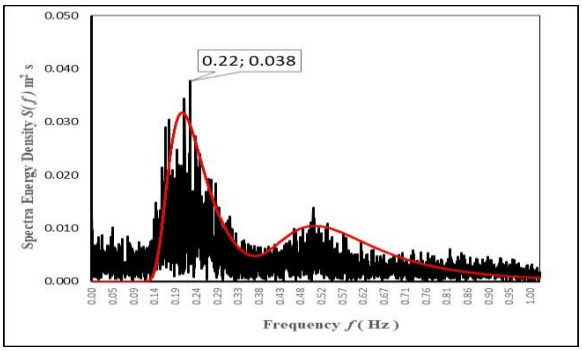


(d)

Figure 12. Results of spectral analysis for (a) Group-1, (b) Group-13, (c) Group-25 and (d) Group-37.

Various studies have described the possibility and mechanism of the appearance of multi-peaks on the wave spectral graphs. The main or highest peak is obviously brought by the contribution of the waves generated by local winds. The second peak is developed by the contributions of swells propagating from remote region of the connected waters (Wang & Hwang 2002; Ewans et al 2006). However, no explanation could be found with respect to the appearance of the third peak.

The spectral analysis was still being conducted at the time of this paper was prepared. The further analysis is expected to produce values of characteristic wave heights and periods that would be correlated with the results of short-term analysis. Ultimately after all the wave spectra curves are attained from the processing of one-year data, a spectral model specifically for the Western Java Sea could be developed.

**Conclusions**. A study on the wave characteristics of Western Java Sea has been conducted by way of direct wave measurement conducted for one full year. Preliminary analysis was performed on the 48 groups of wave data collected within one day on August 13$^{th}$, 2016 by applying the short-term wave statistical method and followed by spectral method. Results of this preliminary study may be concluded as follows:

- the distribution of wave elevations in general follow the theoretical Gaussian distribution, the distribution of wave height generally conforms the theoretical Rayleigh distribution, and the distribution of wave periods is in accordance with theoretical exponential family distribution;
- the distribution of wave elevation, height, and period experience an oscillation during the time elapsed within one day;
- the digital counting of the number of waves from 48 data groups yield the values between 463 and 718 waves;
- the lowest characteristic wave heights of $H_{av}$, $H_{rms}$, $H_s$, and $H_{max}$ are, respectively, 169 mm, 220 mm, 311 mm, and 539 mm. While the highest of those four characteristic wave heights are, correspondingly, 538 mm, 643 mm, 920 mm, and 1788 mm;
- the average wave height ratios of $H_s/H_{av}$ is 1.735, $H_s/H_{rms}$ is 1.422, and $H_{max}/H_s$ is 1.856. These ratios are in conformation with the ranges as suggested by prominent references;
- the computation of average period utilizing four (4) approaches give value ranges between 2.5 and 3.9 seconds;
- the spectral analysis produces spectral curves that specifically exhibit single peak and double peaks. The primary or larger peak represents the energy from local waves, whereas the second or lower peak represents the contribution of swell.

The future work of this study would cover completing monthly wave analysis for overall data collected in 12 months. Finally, formulation of spectral model appropriate for the Western Java Sea would be established.

## References


Azami H., Mohammadi K., Bozorgtabar B., 2012 An improved signal segmentation using moving average and Savitzky-Golay filter. Journal of Signal and Information Processing 3(1):39-44.

Adrianto D., Djatmiko E. B., Suntoyo, 2019 The improvement of ultrasonic sensor-based device for direct ocean wave measurement program at Western Java Sea – Indonesia. Geomatics International Conference 2019. IOP Conferece Series: Earth and Environmental Science 389:012022.

Boccotti P., 2015 Wave mechanics and wave loads on marine structures. Butterworth-Heinemann, Elsevier, Oxford, UK, 344 pp.

Cartwright D. E., Longuet-Higgins M. S., 1956 The statistical distribution of the maxima of the random function. Proceedings of the Royal Society London, Series A 237:212-232.

Chakrabarti S. K., 1987 Hydrodynamics of offshore structures. Computational Mechanics Publications, Springer-Verlag, Berlin, 440 pp.

Cho H. Y., Kweon H. M., Jeong W. M., Kim S. I., 2015 A study on the optimal equation of the continuous wave spectrum. International Journal of Naval Architecture and Ocean Engineering 7(6):1056-1063.
Cooley J. W., Tukey J. W., 1965 An algorithm for the machine calculation of complex Fourier series. Mathematics of Computation 19(90):297-301.
Dai W., Selesnick I., Rizzo J. R., Rucker J., Hudson T., 2017 A nonlinear generalization of the Savitzky-Golay filter and the quantitative analysis of saccades. Journal of Vision 17(9):10.
Denis S. M., Pierson W. J., 1953 On the motions of ships in confused seas. Transactions of SNAME 61:280-357.
Djatmiko E. B., 2012 Perilaku dan operabilitas bangunan laut di atas gelombang acak. ITS Press, Surabaya, 225 pp. [in Indonesian]
Djatmiko E. B., Adrianto D., 2013 Urgency in the establishment of a national sea wave forecasting center to enhance marine disaster prevention and control in Indonesia. International Seminar on Marine, Coastal Engineering, Environmental and Natural Disaster Management, Surabaya, Indonesia, 11 Nov, 14 pp.
Djatmiko E. B., Syahroni N., Sujantoko S., Supomo H., Nugroho S., 2019 Evaluation of articulated tower-ocean wave energy converter (AT-OWEC) – part I: the dynamic behavior under wave excitation. International Review of Mechanical Engineering (IREME) 13(10):568-575.
Ewans K. C., Bitner-Gregersen E. M., Guedes-Soares C., 2006 Estimation of wind-sea and swell components in a bimodal sea state. Journal of Offshore Mechanics and Arctic Engineering 128:265-270.
Fedele F., Benetazzo A., Gallego G., Shih P. C., Yezzi A., Barbariol F., Ardhuin F., 2013 Space-time measurements of oceanic sea state. Ocean Modelling 70:103-115.
Goda Y., 1985 Random seas and design of marine structures. University of Tokyo Press, Tokyo, Japan, 323 pp.
Guedes-Soares C., Carvalho A. N., 2012 Probability distributions of wave heights and periods in combined sea-states measured off the Spanish coast. Ocean Engineering 52:13-21.
Hamilton L. J., 2010 Characterising spectral sea wave conditions with statistical clustering of actual spectra. Applied Ocean Research 32(3):332-342.
Hasselman K., Barnett T. P., Bouws E., et al, 1973 Measurement of wind-wave growth and swell decay during the Joint North Sea Wave Project (JONSWAP). Ergänzungsheft zur Deutschen Hydrographischen Zeitschrift Reihe A(8$^{o}$) Nr. 12, Deutsches Hydrographisches Institut, Hamburg, 95 pp.
Hasselman K., Ross D. B., Muller P., Sell W., 1976 A parametric wave prediction model. Journal of Physical Oceanography 6:200-228.
INHOC, 2010 Map of Indonesia Archipelago and Surround, Western Portion, Indonesian Navy Hydrography and Oceanography Center, Jakarta.
Kun A., Fougere A., McComb P., 1999 A new wave directional spectrum measurement instrument. Proceedings of the IEEE Sixth Working Conference on Current Measurement, San Diego, USA, March, pp. 49-53.
Lin H., Xu Q., Zheng Q., 2008 An overview on SAR measurements of sea surface wind. Progress in Natural Science 18(8):913-919.
Monbet V., Ailliot P., Prevosto M., 2007 Survey of stochastic models for wind and sea state time series. Probabilistic Engineering Mechanics 22(2):113-26.
Murdjito M., Pravitasari I. Y., Djatmiko E. B., 2020 An analysis on the spread mooring of the Belida FSO induced by squall loads. KAPAL: Jurnal Ilmu Pengetahuan dan Teknologi Kelautan 17(1):15-27.
Pierson W. J., Marks W., 1952 The power spectrum analysis of ocean-wave records. Transactions of American Geophysical Union 33(6):834-844.
Ryabkova M., Karaev V., Guo J., Titchenko Y., 2019 A review of wave spectrum models as applied to the problem of radar probing of the sea surface. Journal of Geophysical Research: Oceans 124(10):7104-7134.

Shajeesh K. U., Sachin K. S., Pravena D., Soman K. P., 2012 Speech enhancement based on Savitzky-Golay smoothing filter. International Journal of Computer Aplications 57(21):39-44.
Wang D. W, Hwang P. A., 2002 An operational method for separating wind sea and swell from ocean wave spectra. Journal of Atmospheric and Oceanic Technology 18:2052-2062.
Weisse R., von Storch H., 2009 Marine climate and climate change: storms, wind waves and storm surges. Springer Praxis Books, New York, USA, 219 pp.
Widjiati E., Djatmiko E. B., Wardhana W., Wirawan, 2015 Cavitation noise characterization of two B-series propeller models in the cavitation tunnel. Journal of Engineering and Applied Sciences 10(3):45-57.
Xie B., Ren X., Jia X., Li Z., 2019 Research on ocean wave spectrum and parameter statistics in the northern South China Sea. Offshore Technology Conference, Houston, Texas, 6-9 May, Paper OTC-29547-MS.

Received: 16 February 2020. Accepted: 20 March 2020. Published online: 31 March 2020.
Authors:
Dian Adrianto, Post Graduate Program, Faculty of Marine Technology, Institut Teknologi Sepuluh Nopember (ITS), Surabaya 60111, Indonesia, e-mail: aqilaadrianto@gmail.com
Eko B. Djatmiko, Department of Ocean Engineering, Institut Teknologi Sepuluh Nopember (ITS), Surabaya 60111, Indonesia, e-mail: ebdjatmiko@oe.its.ac.id
Suntoyo, Department of Ocean Engineering, Institut Teknologi Sepuluh Nopember (ITS), Surabaya 60111, Indonesia, e-mail: suntoyo@oe.its.ac.id

How to cite this article:
Adrianto D., Djatmiko E. B., Suntoyo, 2020 The 6-Hz wave measurements in Western Java Sea and its preliminary characteristics analysis. AES Bioflux 12(1):66-82.